Applied Physics Letters ARTICLE scitation.org/journal/apl

Bottom tunnel junction blue light-emitting field-effect transistors

Cite as: Appl. Phys. Lett. **117**, 031107 (2020); doi: 10.1063/5.0009430
Submitted: 30 March 2020 · Accepted: 4 July 2020 ·
Published Online: 24 July 2020

View Online

Export Citation

CrossMark

Shyam Bharadwaj,[1,a)] Kevin Lee,[1] Kazuki Nomoto,[1] Austin Hickman,[1] Len van Deurzen,[2] Vladimir Protasenko,[1] Huili (Grace) Xing,[1,3,4] and Debdeep Jena[1,3,4]

AFFILIATIONS

[1]School of Electrical and Computer Engineering, Cornell University, Ithaca, New York 14853, USA
[2]Department of Applied and Engineering Physics, Cornell University, Ithaca, New York 14853, USA
[3]Department of Material Science and Engineering, Cornell University, Ithaca, New York 14853, USA
[4]Kavli Institute for Nanoscale Science, Cornell University, Ithaca, New York 14853, USA

[a)]Author to whom correspondence should be addressed: sb2347@cornell.edu

ABSTRACT

A recent thrust toward efficient modulated light emitters for use in Li-Fi communications has sparked renewed interest in visible III-N InGaN light-emitting diodes (LEDs). With their high external quantum efficiencies, blue InGaN LEDs are ideal components for such devices. We report a method for achieving voltage-controlled gate-modulated light emission using monolithic integration of fin- and nanowire-n–i–n vertical FETs with bottom-tunnel junction planar blue InGaN LEDs. This method takes advantage of the improved performance of bottom-tunnel junction LEDs over their top-tunnel junction counterparts, while allowing for strong gate control on a low-cross-sectional area fin or wire without sacrificing the LED active area as in lateral integration designs. Electrical modulation of five orders and an order of magnitude of optical modulation are achieved in the device.

Published under license by AIP Publishing. https://doi.org/10.1063/5.0009430

Visible light-emitting diodes (LEDs) based on the Indium Gallium Nitride (InGaN) material system have emerged as fundamental components in micro-LED display technology, car headlamps, and cell phone backlighting, among other lighting applications.[1–7] More recently, interest in InGaN LEDs has spread beyond lighting applications toward a different area—light fidelity (Li-Fi) communications—due to the promise of faster and more secure data transmission compared to conventional Wi-Fi.[8,9] InGaN LEDs are attractive for such applications due to their preponderance in lighting and also due to their high external quantum efficiencies (EQEs) in the visible spectral range—a range that is >2000× larger in bandwidth than the entire RF spectral range and the one that is currently underutilized.[10]

In order to use LEDs for Li-Fi communications, high speed modulation of the LED light output is desirable. This modulation is achieved with the use of a current or voltage driver. In the GaAs semiconductor family, heterojunction bipolar transistors (HBTs) have been redesigned epitaxially into LEDs and even laser diodes (LDs) for current driven operation.[11] Although the Nitride semiconductor family allows for visible to UV emission wavelengths and higher power operation, to realize HBT-LEDs or HBT-LDs similar to GaAs requires the quantum well (QW) active region to be placed inside p-type base layers, which are rather resistive and problematic for contact formation. Voltage-driven control methods involve simpler control schemes and offer more flexibility than current-driven methods.[12–14] Using GaN FETs directly integrated on the LED for voltage driving can take advantage of a single epitaxial step and the excellent performance demonstrated by vertical GaN FETs. Toward this end, integration of GaN-based FETs and LEDs on the same epi-wafer can enable high power and high efficiency voltage-controlled modulated visible light emission while eliminating interconnects and reducing the overall device footprint. Previous demonstrations integrating III-Nitride FETs and LED structures on the same epi-wafer for these applications involve lateral integration of High Electron Mobility Transistors (HEMTs) with the LED or vertical integration through a top-down full nanowire platform.[15–23] However, both strategies limit the LED active area on the wafer: the former strategy requires removing the LED epi from certain regions of the wafer (and in certain processes, an additional regrowth step to define the LED structure). The latter constrains the LED active volume down to the size of a gate-controllable nanowire, severely limiting the optical output power. The strategy demonstrated in this work offers a solution to both problems by integrating nanowire and fin vertical n-FETs on large-area planar LEDs

through top-down fabrication on a heterostructure that is realized in one epitaxial stack. This approach allows for strong all-around gate control on the relatively low cross-sectional area FETs, while allowing large area LEDs that take advantage of the on-wafer area for high output power.

In order to vertically integrate nanowire- or fin-n-FETs with planar LEDs, the wires or fins must sit on top of the planar LED. This requires the top layer of the LED to be n-GaN rather than p-GaN. A tunnel junction (TJ) LED is required if conventional n-GaN substrates are used. This particular demonstration uses bottom-TJ homojunction LEDs, which have been shown to outperform standard top-TJ LEDs in terms of wall-plug efficiency,[24,25] with n–i–n vertical n-FETs on top, as shown in Fig. 1, with a circuit level schematic of light-emitting FET (LEFET) devices shown in Fig. 1(d).

The light-emitting FET (LEFET) structure was grown by plasma-assisted molecular beam epitaxy (PAMBE) in a single growth on a free standing Lumilog bulk n-type GaN substrate with a dislocation density of 10^7 cm^{-2}. The growth was performed using a Nitrogen RF plasma power of 400 W, corresponding to a growth rate of 420 nm/h. During growth, reflection high-energy electron diffraction (RHEED) was used to confirm a metal-rich growth condition, which promotes 2D growth in PAMBE.

The epitaxial layer structure of the sample is shown in Fig. 1(a). The initial 125 nm n^+GaN:Si layer was grown at a thermocouple temperature of 750 °C with a Si beam equivalent pressure (BEP) of 3.8×10^{-10} Torr. This BEP corresponds to a Si donor concentration of 1.6×10^{19} cm^{-3}, as calibrated by secondary ion mass spectrometry (SIMS) on a separate sample. The substrate temperature was then reduced to 745 °C to grow the 167 nm p^+GaN:Mg layer in order to enhance Mg incorporation. Mg BEP was kept at 2.3×10^{-8} Torr, corresponding to a Mg acceptor concentration of 2×10^{19} cm^{-3}. After growing p^+GaN:Mg, the growth was interrupted to desorb excess Ga prior to active region growth. The active region consists of three 17% InGaN quantum wells (QWs) separated by 13% InGaN quantum barriers (QBs), all grown at a lower temperature of 657 °C to enhance Indium incorporation. After the active region, a 150 nm n^+GaN layer is grown followed by 600 nm of unintentionally doped (UID) GaN as the channel for the FET. Finally, a 50 nm degenerately doped n^{++}GaN ([Si] = 1×10^{20} cm^{-3}) layer was grown as the source n-contact layer for the transistor.

Optical microscope images after the MBE growth showed Ga metal droplets on the surface, confirming the metal rich growth condition. After removing the droplets with HCl, structural characterization was performed through x-ray diffraction (XRD) and atomic force microscopy (AFM), with the results shown in Figs. 2(a) and 2(b), respectively. The XRD shows that the InGaN cladding composition in the LED is 13%, and the AFM shows a smooth surface (with a root mean square roughness of ~0.6 nm). After performing structural characterization, the sample was processed into devices consisting of various numbers of vertical n-FET nanowires or fins of varying dimensions on top of 55 × 55 μm^2 LED mesas, in a similar manner to other GaN and Ga_2O_3 vertical FETs.[26–28] A schematic of a processed nanowire LEFET is shown in Fig. 1(b). First, 55 × 55 μm^2 LED areas were isolated through inductively coupled plasma reactive ion etching (ICP-RIE) down to the n^+GaN nucleation layer. Next, nanowires and fins were defined on the mesa surface through electron beam lithography (EBL). The etch process for nanowire/fin definition consisted of first an ICP etch (using Cr/Pt as an etch mask as well as a top source contact) followed by a wet etch in AZ400K to make the sidewalls vertical for efficient lateral gating [see Fig. 1(c)]. The fins were defined with the long edge along the m-plane direction in order to allow for adequate wet etching. Then, SiO_2 was deposited by atomic layer deposition (ALD) as a gate dielectric for the nanowire/fin FETs. Next, Cr was sputtered as the sidewall gate metal, followed by e-beam evaporation of large Cr/Au/Ni pads for electrically contacting the gate. The undesired sputtered Cr above the source contact of the fins and wires was etched away after a planarization process, after which SiO_2 was blanket deposited by plasma-enhanced chemical vapor deposition (PECVD)

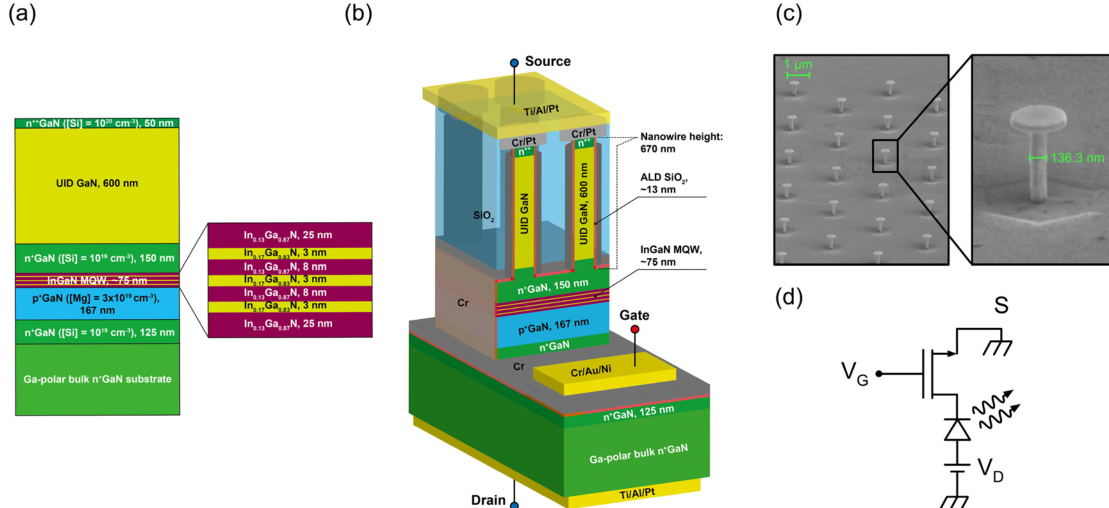

FIG. 1. (a) Epitaxial layer structure for the Light-Emitting FET (LEFET). The structure consists of a vertical n–i–n GaN FET sitting above a bottom-TJ homojunction InGaN LED. (b) Schematic of a fabricated nanowire LEFET structure, showing source, gate, and drain contacts for biasing the device, and dielectrics for isolation. (c) SEM image showing submicrometer nanowires with vertical sidewalls after wet etching, before removing the etch mask. (d) Circuit level schematic of the LEFET.

Published under license by AIP Publishing

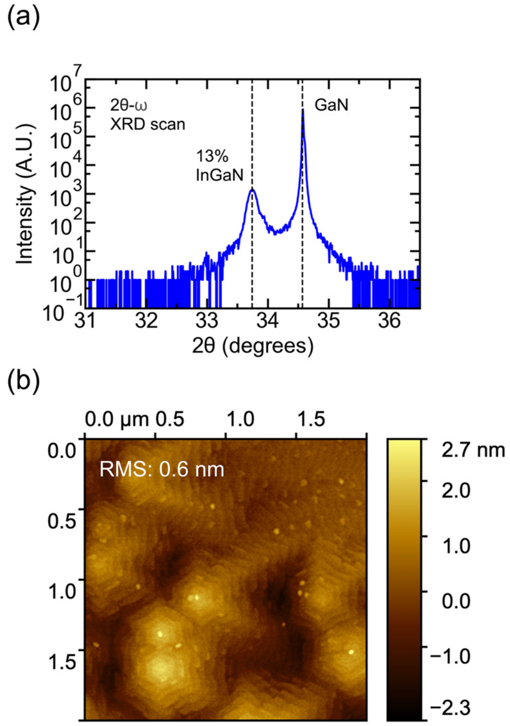

FIG. 2. (a) X-ray diffraction spectrum for the LEFET structure, showing a GaN substrate peak and an $In_{0.13}Ga_{0.87}N$ peak from the LED cladding regions. (b) 2 × 2 μm^2 AFM scan for the structure in this study immediately after MBE growth. Atomic steps and relatively low RMS roughness are observed, with some threading dislocation features present due to propagation from the substrate.

to isolate the rest of the sidewall gate metal. This SiO_2 was then planarized to again expose the Cr/Pt wire/fin source contact, after which thick source pads (Ti/Al/Pt) for probing were deposited. Gate isolation for the FET wires/fins between different devices (which still had their gates shorted together by the sputtered Cr at this point) and contact holes for the thick gate pads was realized together with an SiO_2 etch followed by a Cr etch. Finally, a Ti/Al/Pt back contact was deposited with a window left free of metal for collecting light from the back side.

After device processing, electrical and optical measurements were performed, with the results for a 500 nm × 50 μm single-fin depletion-mode device shown in Figs. 3 and 4, respectively. Compared to the multi-fin/wire devices, the single fin/wire devices showed lower gate leakage current and higher on/off ratios due to the reduced gate area. Circular transfer length method (cTLM) measurements shown in Fig. 3(a) reveal low contact and sheet resistances of 9.34×10^{-6} Ω cm^2 for the top source contact and 185 Ω/sq for the n^{++}GaN contact layer underneath, resulting in negligible voltage drops across these regions. I_D–V_G and I_D–V_D measurements on the 500 nm × 50 μm single-fin device are shown in Figs. 3(b) and 3(c), respectively, with current density values shown on the plots normalized to the area of the fin FET. From the I_D–V_G curve in Fig. 3(b), an on/off ratio of ~5 orders is observed up to $V_{DS} = 4$ V, with gate leakage current low in all cases (below ~100 pA). The on current increases with increasing V_{DS} as expected due to the turn-on of the LED pn diode. The I_D–V_D measurements in Fig. 3(c) show that

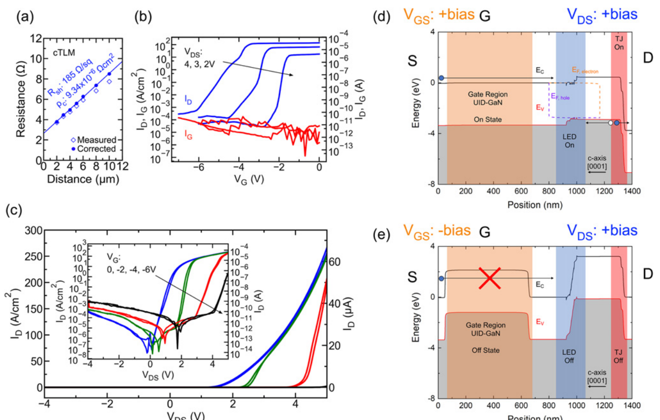

FIG. 3. (a) Circular TLM data for the source contact of the LEFET. (b) I_DV_G measurement for a single-fin device with fin dimensions of 500 nm × 50 μm and LED dimensions of 55 × 55 μm^2. Current density is calculated using the area of the fin. (c) Linear I_DV_D characteristic (with the log scale in the inset) showing reduction in on current of ~100× at $V_{DS} = 5$ V as V_G is reduced from 0 V to −6 V. (d) and (e) Qualitative depiction of band diagrams for the device in the on and off states, respectively. With a fixed positive V_{DS}, switching V_G from positive to negative biases modulates electron conduction across the FET channel and allows voltage to drop across the diode.

between $V_G = 0$ V and $V_G = -6$ V, a two order gate modulation of the on current is achieved at $V_{DS} = +5$ V. Figures 3(e) and 3(f) depict the energy band diagrams of the LEFET device in the on and off states, respectively, when biased in a manner applicable for Li-Fi purposes: modulating V_G with fixed forward bias V_{DS}. In ideal operation,

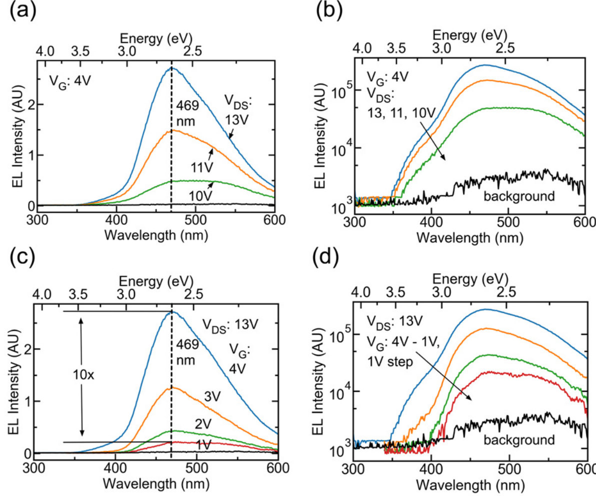

FIG. 4. (a) and (b) Linear and log scale plots, respectively, of electroluminescence (EL) intensity vs wavelength for a single-fin device, with V_G fixed at +4 V. The EL intensity rises as expected with increasing V_{DS} as the level of forward bias across the diode is increased. (c) and (d) Linear and log scale plots, respectively, of EL intensity vs wavelength for the same device, with V_{DS} fixed at 13 V. A factor of 10 reduction in EL intensity is observed as V_G is decreased from +4 V to +1 V, demonstrating the gate's ability to limit electron transport into the LED. At $V_G = 0$ V, light is still emitted although, at a low intensity, the detector is not sensitive enough to resolve.

Published under license by AIP Publishing

electrons are injected into the LED portion of the device from the transistor source only when V_G is switched to a sufficiently high positive voltage.

The measured electroluminescence (EL) spectra are shown in Fig. 4, demonstrating the optical modulation enabled by the FinFET. Figures 4(a) and 4(b) show the effect of the drain voltage on the emission spectra on linear and log scales for the 500 nm × 50 μm single fin device at a fixed $V_G = 4$ V for V_{DS} between 10 V and 13 V. With larger V_{DS}, more light is emitted from the device due to a larger forward bias appearing across the LED portion of the device. V_{DS} used here is higher than that in the electrical measurements due to the limited sensitivity of the optical detection setup used for this work. The emission peak appears at 469 nm, consistent with a 17% average Indium composition in the QWs.

Figures 4(c) and 4(d) demonstrate the desired modulation of the EL spectra through gating of the GaN FinFET. At a fixed $V_{DS} = 13$ V, varying V_G from +4 V to +1 V results in a reduction of EL intensity by a factor of 10. Larger on/off modulation ratios are achieved at lower V_{DS} although the optical measurement apparatus used is not sensitive enough to measure them. Gate control is limited at these high V_{DS} values at which light can be collected by the detector due to the high gate–drain field. The brightness of the LED at lower V_{DS} can be drastically increased through the use of a heterojunction GaN/InGaN/GaN buried tunnel junction rather than a homojunction, leading to a lower series resistance, as demonstrated in previous work.[25] Such devices show strong EL at current densities of ~1 kA/cm^2 (corresponding to ~5 V)—a V_{DS} voltage/field at which the FET portion of this device shows ~5 orders of on/off ratio. Additionally, increasing the thickness of the n^+GaN layer between the fin-FET and planar LED active region will enhance current spreading, increasing optical output power.

For visible light communications, switching speed is an important parameter that dictates data transmission rates. The optical switching speed of the device was measured by switching V_G with V_{DS} fixed at 10 V and tracking the output signal from a photodiode placed directly underneath the device using an oscilloscope. A square voltage pulse with a duty cycle of 50% was used as the input signal on the gate, with the frequency varying between 1 kHz and 100 kHz. The input electrical signal (black) and output photodiode voltage signal (red) are shown in Fig. 5 for frequencies of 10 and 30 kHz. Limitations of the optical collection setup result in a low signal to noise ratio, and so a Savitzky–Golay filter was used after collecting the data to reduce the noise in the photodiode output signal. The device maintains an optical switching response up to 30 kHz, beyond which the optical response flattens out. Although this modulation proves the feasibility of the LEFET for direct voltage modulation of light, the current design of the device geometry is not optimal for the much higher speeds necessary. Future designs will require careful control of the UID GaN thickness and the sidewall gate dielectric and the resulting gate capacitance to enhance the gate-voltage modulation speed of the optical output power.

We have demonstrated a technique for achieving monolithic integration of n-FETs and LEDs, using vertical fin- and nanowire-FETs and bottom tunnel junction planar blue LEDs. This platform allows for strong gate control (~5 orders of magnitude on/off for I_D) without limiting the on-wafer LED active area and does not require regrowth. Optical switching behavior up to 30 kHz is demonstrated in the first prototype, with room for improvement through the use of

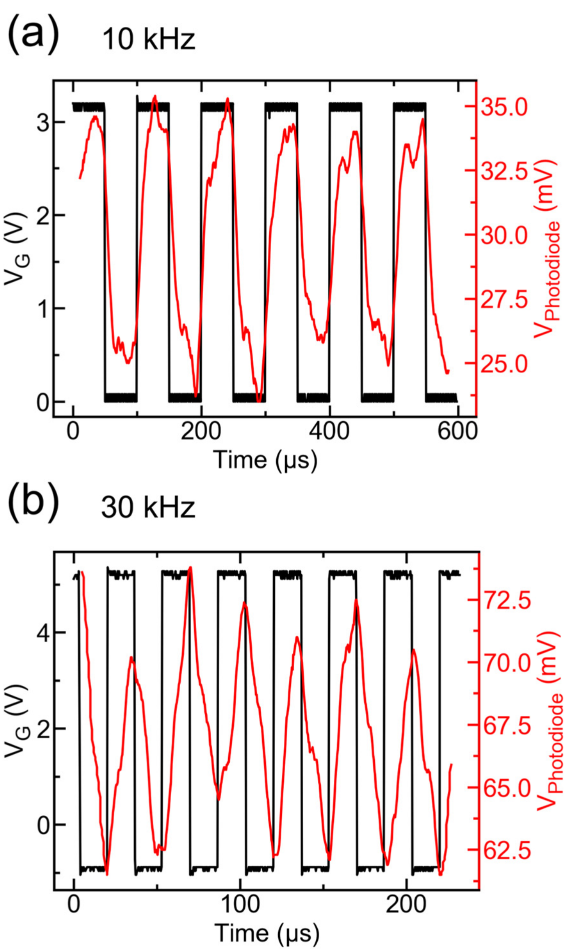

FIG. 5. (a) and (b) Switching measurements performed on the 500 nm × 50 μm single fin device with a 50% duty cycle square wave applied to the gate at frequencies of 10 kHz and 30 kHz, respectively. For the 10 kHz measurement, V_G is switched from 0 to +3 V, while for the 30 kHz measurement, V_G is switched from −1 V to +4 V. V_{DS} is held constant at 10 V for both measurements. The black signal denotes the input voltage V_G, while the red signal is the response measured by a photodiode placed ~2 cm away from the sample. A Savitzky–Golay filter was used to reduce noise in the photodiode response.

InGaN heterojunction TJs. The LEFET device geometry can be easily modified for light extraction from the surface without sacrificing significant wafer area by patterning the top source contact. Such devices are promising for use in Li-Fi communications and in micro-LED displays, in which gate voltage controllability and utility of space are important parameters. The technique described here can be applied to integrate vertical fin-FETs with laser diodes, enabling efficient directional Li-Fi emitters among other technologies.

This work was supported in part by the following National Science Foundation (NSF) grants: NSF DMREF Award No. 1534303 monitored by Dr. J. Schluter, NSF Award No. 1710298 monitored by Dr. T. Paskova, NSF CCMR MRSEC Award No. 1719875, and NSF RAISE TAQs Award No. 1839196 monitored by Dr. D. Dagenais. This work made use of the shared facilities that are supported through the

Published under license by AIP Publishing

NSF National Nanotechnology Coordinated Infrastructure (Grant No. ECCS-1542081) and NSF MRSEC program (No. DMR-1719875) and No. MRI DMR-1338010.

DATA AVAILABILITY

The data that support the findings of this study are available from the corresponding author upon reasonable request.

REFERENCES

[1]P. Tian, J. J. D. McKendry, E. Gu, Z. Chen, Y. Sun, G. Zhang, M. D. Dawson, and R. Liu, "Fabrication, characterization and applications of flexible vertical InGaN micro-light emitting diode arrays," Opt. Express **24**, 699 (2016).
[2]L. Dupré, M. Marra, V. Verney, B. Aventurier, F. Henry, F. Olivier, S. Tirano, A. Daami, and F. Templier, "Processing and characterization of high resolution GaN/InGaN LED arrays at 10 micron pitch for micro display applications," in Gallium Nitride Materials and Devices XII (2017), Vol. 10104, p. 1010422.
[3]K.-J. Pai, "Temperature rise effects on dynamic resistances for laser diodes with a wavelength of 450 nm for vehicle headlight applications," IEEE Trans. Veh. Technol. **68**, 9529–9521 (2019).
[4]M. Anandan, "Progress of LED backlights for LCDs," J. Soc. Inf. Disp. **16**, 287 (2008).
[5]S. P. Denbaars, D. Feezell, K. Kelchner, S. Pimputkar, C. C. Pan, C. C. Yen, S. Tanaka, Y. Zhao, N. Pfaff, R. Farrell *et al.*, "Development of gallium-nitride-based light-emitting diodes (LEDs) and laser diodes for energy-efficient lighting and displays," Acta Mater. **61**, 945–951 (2013).
[6]S. Nakamura, T. Mukai, and M. Senoh, "Candela-class high-brightness InGaN/AlGaN double-heterostructure blue-light-emitting diodes," Appl. Phys. Lett. **64**, 1687–1689 (1994).
[7]K. A. Denault, M. Cantore, S. Nakamura, S. P. Denbaars, and R. Seshadri, "Efficient and stable laser-driven white lighting," AIP Adv. **3**, 072107 (2013).
[8]H. Li, X. Chen, J. Guo, and H. Chen, "A 550 Mbit/s real-time visible light communication system based on phosphorescent white light LED for practical high-speed low-complexity application," Opt. Express **22**, 27203 (2014).
[9]C. L. Tsai and Z. F. Xu, "Line-of-sight visible light communications with InGaN-based resonant cavity LEDs," IEEE Photonics Technol. Lett. **25**, 1793–1796 (2013).
[10]H. Haas, "LiFi is a paradigm-shifting 5G technology," Rev. Phys. **3**, 26–31 (2018).
[11]M. Feng, N. Holonyak, G. Walter, and R. Chan, "Room temperature continuous wave operation of a heterojunction bipolar transistor laser," Appl. Phys. Lett. **87**, 131103–131103 (2005).
[12]Y. R. Yang, "Brightness control of LED lamps using fuzzy logic controllers," in Proceedings of the 2010 5th IEEE Conference on Industrial Electronics and Applications, ICIEA 2010 (2010), pp. 1957–1962.
[13]J. Garcia, D. G. Lamar, M. A. Dalla-Costa, J. M. Alonso, and M. Rico-Secades, "An estimator of luminous flux for enhanced control of high brightness LEDs," in PESC Record—IEEE Annual Power Electronics Specialists Conference (2008), pp. 1852–1856.
[14]A. I. Bogdan and N. Bizon, "Voltage-mode control of the DC-DC power converter: A short review," in Proceedings of the 2015 7th International Conference on Electronics, Computers and Artifical Intelligence (ECAI) (2015), pp. E27–E32.
[15]Y. Cai, X. Zou, C. Liu, and K. M. Lau, "Voltage-controlled GaN HEMT-LED devices as fast-switching and dimmable light emitters," IEEE Electron Device Lett. **39**, 224–227 (2018).
[16]M. Hartensveld and J. Zhang, "Monolithic integration of GaN nanowire light-emitting diode with field effect transistor," IEEE Electron Device Lett. **40**, 427–430 (2019).
[17]Z. Li, J. Waldron, T. Detchprohm, C. Wetzel, R. F. Karlicek, and T. P. Chow, "Monolithic integration of light-emitting diodes and power metal-oxide-semiconductor channel high-electron-mobility transistors for light-emitting power integrated circuits in GaN on sapphire substrate," Appl. Phys. Lett. **102**, 192107 (2013).
[18]J. Yan, J. Piao, and Y. Wang, "An enhancement mode MOSFET based on GaN-on-silicon platform for monolithic OEIC," IEEE Electron Device Lett. **41**, 76–79 (2020).
[19]C. Liu, Y. Cai, Z. Liu, J. Ma, and K. M. Lau, "Metal-interconnection-free integration of InGaN/GaN light emitting diodes with AlGaN/GaN high electron mobility transistors," Appl. Phys. Lett. **106**, 181110 (2015).
[20]Z. Guo, M. Bulsara, T. Paul Chow, C. Hitchcock, C. Wetzel, R. F. Karlicek, G. Piao, Y. Yano, S. Koseki, T. Tabuchi *et al.*, "Monolithically integrated GaN LED/quasi-vertical power U-shaped trench-gate MOSFET pairs using selective epi removal," IEEE Electron Device Lett. **40**, 1736–1739 (2019).
[21]H. Electrode, "Low-leakage high-breakdown laterally integrated," IEEE Photonics Technol. Lett. **28**, 1130–1133 (2016).
[22]C. Y. Chang, Y. C. Li, K. Ren, Y. C. Liang, and C. F. Huang, "An AlGaN/GaN high electron mobility transistor with a built-in light emitter using radiative recombination of two-dimensional electron gas and holes," IEEE J. Electron Devices Soc. **8**, 346–349 (2020).
[23]Z. Guo, C. Hitchcock, R. F. Karlicek, G. Piao, Y. Yano, S. Koseki, T. Tabuchi, K. Matsumoto, M. Bulsara, and T. P. Chow, "Integrable quasivertical GaN U-shaped trench-gate metal-oxide-semiconductor field-effect transistors for power and optoelectronic integrated circuits," Phys. Status Solidi A **217**, 2070026–2070028 (2020).
[24]H. Turski, S. Bharadwaj, H. Xing, and D. Jena, "Polarization control in nitride quantum well light emitters enabled by bottom tunnel-junctions," J. Appl. Phys. **125**, 203104 (2019).
[25]S. Bharadwaj, J. Miller, K. Lee, J. Lederman, M. Siekacz, H. G. Xing, D. Jena, C. Skierbiszewski, and H. Turski, "Enhanced injection efficiency and light output in bottom tunnel-junction light-emitting diodes using UID GaN spacers," Opt. Express **28**, 4489–4500 (2020).
[26]Z. Hu, W. Li, K. Nomoto, M. Zhu, X. Gao, M. Pilla, D. Jena, and H. G. Xing, "GaN vertical nanowire and fin power MISFETs," in Device Research Conference-Conference Digest, DRC (2017), Vol. 35.
[27]Z. Hu, K. Nomoto, W. Li, Z. Zhang, N. Tanen, Q. T. Thieu, K. Sasaki, A. Kuramata, T. Nakamura, D. Jena *et al.*, "Breakdown mechanism in 1 kA/cm^2 and 960 v E-mode β-Ga_2O_3 vertical transistors," Appl. Phys. Lett. **113**, 122103–122108 (2018).
[28]W. Li, K. Nomoto, Z. Hu, T. Nakamura, D. Jena, and H. G. Xing, "Single and multi-fin normally-off Ga_2O_3 vertical transistors with a breakdown voltage over 2.6 kV," in Technical Digest-International Electron Devices Meeting, IEDM, December (2019), pp. 270–273.

Published under license by AIP Publishing